

Adsorption characteristics of Ni(II) onto MA–DTPA/PVDF chelating membrane

Xiaodan Zhao, Laizhou Song*, Jie Fu, Pei Tang, Feng Liu

Department of Environmental and Chemical Engineering, Yanshan University, Qinhuangdao 066004, China

ARTICLE INFO

Article history:

Received 10 December 2010
Received in revised form 23 February 2011
Accepted 16 March 2011
Available online 23 March 2011

Keywords:

PVDF chelating membrane
Adsorption
Nickel–organic complexes
Kinetics
Isotherm

ABSTRACT

The melamine–diethylenetriaminepentaacetic acid/polyvinylidene fluoride (MA–DTPA/PVDF) chelating membrane bearing polyaminocarboxylate groups was prepared for the removal of Ni(II) from wastewater effluents. The membrane was characterized by SEM, ¹³C NMR and FTIR techniques. Quantitative adsorption experiments were performed in view of pH, contact time, temperature, the presence of Ca(II) and lactic acid as the controlling parameters. Adsorption kinetics and equilibrium were examined regarding the single Ni(II) system, binary Ni(II) and Ca(II) system and nickel–lactic acid complexes system. The desorption efficiency was also evaluated, and the adsorption mechanism was suggested based on experimental data. The results show that the sorption kinetics fit well to Lagergren second-order equation and the isotherms can be well described by Langmuir model. At 298 K, the second-order rate constant is calculated to be 4.171, 11.39, 6.203 cm²/(mg min) and the equilibrium uptake is 0.0264, 0.0211 and 0.0216 mg/cm² in the aforementioned three systems. The distribution coefficient of Ni(II) slowly decreases from 4.27 to 2.72, and the separation factor ($f_{\text{Ni(II)/Ca(II)}}$) increases from 3.10 to 8.46 when the initial Ca(II) concentration varies from 20 to 200 mg/L. This reveals the chelating membrane shows more affinity for Ni(II) than Ca(II) ions. In the studied range of lactic acid concentration, Ni(II) uptake decreases with the maximum ratio of 10%. Chemical bonding (chelation) dominates in the adsorption process, and the negative ΔG° and ΔH° indicate the spontaneous and exothermic nature of adsorption.

Crown Copyright © 2011 Published by Elsevier B.V. All rights reserved.

1. Introduction

Water contamination by heavy metals has emerged as a crucial problem for environmental considerations. Emission of the wastewater effluents containing heavy metal ions has significantly toxic influences on human beings and ecological systems [1,2]. The amount of the discharged toxic heavy metals including arsenic, mercury, lead, copper, nickel, chromium and cadmium every year can attain millions of tons. Among these metals, there is a significant contamination of water resources by nickel ions [3]. Nickel electroless plating and electroplating industries discharge a large amount of wastewater in China, which has posed a threat to the ecosystem. Nickel has been identified as a carcinogen; therefore, nickel containing wastewater should be treated to maintain legislative standards. Furthermore, the existent form of nickel is metal–organic complexes and citric, lactic, tartaric, malic and succinic acids are found to be widely used in the nickel plating processes. It is thereby not effective for the conventional techniques to recover nickel from complex wastewaters.

Conventional treatment methods include coagulation and filtration [4,5], adsorption [6–9], ion exchange and electro dialysis

[10]. Among these methods, adsorption is recommended for the treatment of wastewater in which metal ions are at low concentration levels. Numerous adsorbents, such as activated carbon, minerals, resins and membranes, are available for heavy metal removal and recovery [11,12]. Activated carbon can efficiently decrease the content of heavy metals complexed by organic acids; however, the regeneration is difficult and thus this adsorbent is not cost-effective [13]. Various ion exchangers are distinguished by their functional groups, determining the different affinity and selectivity for heavy metals. Acrylic acid, crotonic acid, nitrilotriacetic acid and maleic anhydride have been introduced into polymer matrix [14–16]. These common ion exchange adsorbents can be used to remove heavy metals from aqueous solutions, while they cannot perform their functions for metal–organic solutes. Due to the stability of metal complexes, the recovery of nickel from metal plating faces challenges. Membrane techniques, especially the chelating membrane, have found applications in the heavy metal polluted wastewater [6,17]. Also, there are strong complexing agents including ethylenediamine tetra-acetic acid (EDTA) and diethylenetriaminepentaacetic acid (DTPA), which are adopted to functionalize the polymeric materials for heavy metal recovery [18–21]. However, there have been scarce investigations in relation to the modification of polyvinylidene fluoride (PVDF) membrane with DTPA.

In this study, MA–DTPA/PVDF chelating membrane was synthesized via the covalent amide bond between DTPA and melamine

* Corresponding author. Tel.: +86 3358387741; fax: +86 3358061569.
E-mail address: songlz@ysu.edu.cn (L. Song).

(MA) with the formation of polyaminocarboxylate compounds. Scanning electron microscopy (SEM), ^{13}C nuclear magnetic resonance spectroscopy (^{13}C NMR) and Fourier transform infrared spectroscopy (FTIR) were used to characterize the prepared membrane. The chelating membrane was applied to remove nickel from nickel–organic complexes in simulated wastewater. As a preliminary work, lactic acid was chosen as the studied chelating agent for the nickel–organic complexes system. Detailed studies regarding the effects of different parameters including pH, temperature, contact time, the presence of calcium ions and lactic acid on the adsorption properties of the membrane have been carried out. In order to have an insight into the fundamental information of the adsorption process, batch adsorption experiments with respect to the kinetics and isotherms were performed with the presence of calcium ions and lactic acid, respectively. Finally, the experimental data were compared to the adsorption data of single nickel ions to interpret the results.

2. Experimental

2.1. Materials

PVDF powders were provided by Chen Guang Co. Ltd. (China) with a molecular weight of ca. 400,000. Polyvinyl pyrrolidone (PVP) powders, as the pore-forming additive, were obtained from the Institute of Chemical Engineering of Beijing (China). Dimethylsulfoxide (DMSO), DTPA, MA, lactic acid and CaCl_2 were of analytical grade and used as received. A stock solution of Ni(II) (1000 mg/L) was prepared by dissolving weighed amounts of $\text{NiSO}_4 \cdot 6\text{H}_2\text{O}$ (analytical grade) in deionised water. The working solutions were prepared by diluting the stock solutions to appropriate volumes.

2.2. Preparation of the PVDF chelating membrane

DTPA (1.5 g) and melamine (1.44 g) were mixed in 30 mL DMSO. The mixture was then heated to 180°C to form the covalent amide bond between DTPA and MA. When a homogenous suspension was observed, this suspension was cooled to 80°C . At the same time, PVDF (5 g) and PVP (0.7 g) were added to this suspension and then agitated for 5 h with the temperature in range of $70\text{--}80^\circ\text{C}$. The PVDF chelating membrane was obtained via phase inversion technique with deionised water as the nonsolvent. To completely leach out the remaining solvent and PVP, the membrane was immersed in deionised water for 48 h at room temperature and left for subsequent characterization and adsorption experiments.

2.3. Membrane characterization

Environmental scanning electron microscopy (Model XL30, Philips) was employed to analyze the surface morphologies of the virgin PVDF membrane and the chelating membrane. BRUKER AVANCE III 400 NMR spectrometry (^{13}C solid-state NMR) was used to characterize the membrane samples.

Fourier transform infrared spectroscopy was adopted to determine the functional groups of the PVDF chelating membrane. In particular, the FTIR spectrum of nickel-loaded chelating membrane will provide some evidence about the complexing groups and administer to revealing the complexation mechanism. Considering the possible effects of PVDF polymer on the peaks after complexation, FTIR spectra of the polyaminocarboxylate compounds and their nickel-loaded form were also examined. FTIR analyses were conducted on E55 + FRA106 FTIR spectrometer. Each spectrum was collected by cumulating 16 scans at a resolution of 4 cm^{-1} .

2.4. Adsorption experiments

All the following adsorption experiments were performed by a batch method in which 200 mL solutions containing Ni(II) were treated by the chelating membrane with the diameter of 10 cm. The solutions were pH-adjusted using HAC–NaAc buffer solutions.

The effect of pH ranging from 2 to 7.5 was examined. In industrial wastewaters, there exists a large amount of calcium ions in addition to heavy metal ions. In order to elucidate the interference of calcium ions, the nickel uptakes were measured at different Ca(II) concentrations (0–200 mg/L). Lactic acid was chosen as the target chelating agent for studying the removal of nickel in the form of metal–organic complexes. Considering the practical condition of the nickel plating wastewater, the concentration of lactic acid varied from 0 to 10 mL/L. Solutions containing 50 mg/L nickel ions, of which the temperature was kept at 298 K, were used in the above experiments. Furthermore, the optimum pH for adsorption derived from the experimental results of pH effect was adopted for all experiments.

Adsorption kinetics and the effect of contact time were investigated in a series of experiments at three temperatures (288 K, 298 K and 308 K). The initial Ni(II) concentration was also 50 mg/L and pH of the solutions was maintained at 6.6. For each temperature, 1 mL was withdrawn from the solution to determine the residual Ni(II) concentrations at different intervals till equilibrium. In addition, kinetics with the presence of calcium ions and lactic acid were studied, respectively. The Ca(II) concentration was controlled at 50 mg/L. For the kinetics with the addition of lactic acid, the concentration of 0.01 mol/L was employed.

For single Ni(II) aqueous solutions, the effect of temperature (288 K, 298 K and 308 K) and adsorption equilibrium were examined in one experiment at different initial nickel concentrations (20–140 mg/L). The initial and equilibrium concentrations were then measured by atomic absorption spectroscopy (AAS, WFX-110 spectrometer). Adsorption isotherm studies with regard to the existence of calcium ions and lactic acid were carried out by the same method as that of the single nickel ions system. The amounts of calcium ions and lactic acid were the same with the kinetics studies.

The amounts of nickel adsorbed on the chelating membrane, and the distribution coefficient (K_D , mL/cm 2) and separation factor ($f_{\text{Ni(II)/Ca(II)}}$) for nickel and calcium ions were calculated as follows[22]:

$$q = \frac{(c_0 - c_e)V}{A} \quad (1)$$

$$K_D = \frac{(c_0 - c_e)}{c_e} \times \frac{V}{A} \quad (2)$$

$$f_{\text{Ni(II)/Ca(II)}} = \frac{K_{D(\text{Ni})}}{K_{D(\text{Ca})}} \quad (3)$$

where q is the amount of Ni(II) and Ca(II) ions adsorbed onto a unit area of the membrane (mg/cm 2). c_0 and c_e are the initial and equilibrium concentrations of Ni(II) and Ca(II) ions in the aqueous phase (mg/L), respectively. V is the volume of the aqueous phase (L) and A is the surface area of the membrane (cm 2). $K_{D(\text{Ni})}$ and $K_{D(\text{Ca})}$ are the distribution coefficients (L/m 2) of Ni(II) and Ca(II) ions at adsorption equilibrium between the chelating membrane and the solution (mg/L), respectively. $f_{\text{Ni(II)/Ca(II)}}$ is the separation factor of nickel and calcium ions, and $f_{\text{Ni(II)/Ca(II)}}$ with a higher value will benefit the Ni(II) adsorption of the chelating membrane.

2.5. Desorption experiments

Desorption efficiency of the chelating membrane was measured with HCl solution as the elution agent. The chelating membrane with the diameter of 10 cm loaded by the nickel ions was immersed

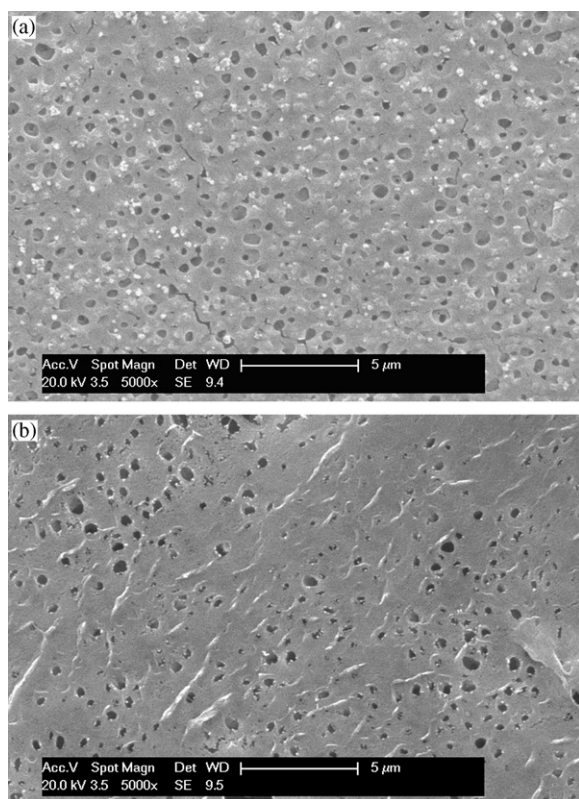


Fig. 1. SEM images of PVDF membrane: (a) surface of the virgin PVDF membrane; (b) surface of the chelating membrane.

in 1 mol/L HCl solution. The adsorption/desorption processes for the same membrane were repeated for four times. The amounts of Ni(II) adsorbed and eluted during the adsorption/desorption processes were determined and the desorption efficiency was then evaluated.

The desorption efficiency (*DE*) was expressed below:

$$DE = \frac{q_1}{q_0} \times 100\% \quad (4)$$

where q_1 is the desorbed amount of Ni(II) ions from the membrane (mg/cm^2) and q_0 is the adsorbed amount of Ni(II) ions on the membrane at equilibrium (mg/cm^2).

3. Results and discussion

3.1. Characterization of the chelating membrane

3.1.1. SEM analysis

Surface morphology of MA–DTPA/PVDF chelating membrane was characterized by SEM. Fig. 1 presents the SEM images of the virgin PVDF membrane and the chelating membrane. As shown in Fig. 1a, the virgin PVDF membrane possesses a uniform microporous structure [23]. In comparison, it can be seen from Fig. 1b that the PVDF chelating membrane still maintains its microstructure; nevertheless this porous microstructure is found to be partially blocked and the porosity tends to decrease. This phenomenon can be attributable to the resultant colloidal substances during the preparation process. The morphology of the PVDF chelating membrane evidences that the polyaminecarboxylate colloid do not have a considerable influence on the micropore structure of PVDF membrane.

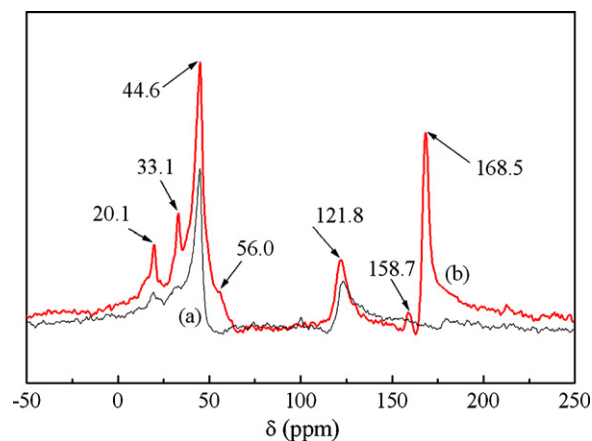


Fig. 2. ^{13}C solid-state NMR spectra: (a) the virgin PVDF membrane; (b) the chelating membrane.

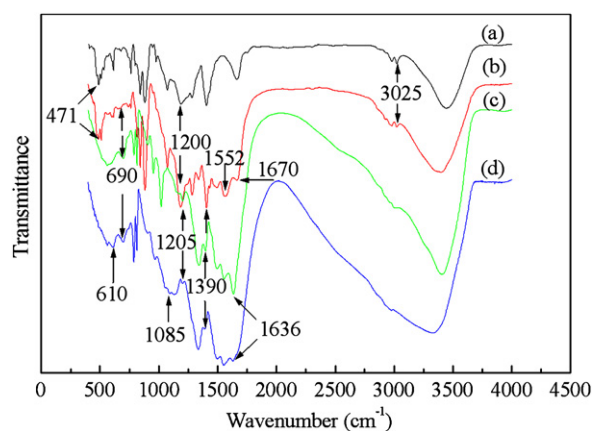


Fig. 3. FTIR spectra: (a) the virgin PVDF membrane; (b) the chelating membrane; (c) polyaminecarboxylate compounds; (d) nickel-loaded polyaminecarboxylate compounds.

3.1.2. NMR analysis

^{13}C solid-state NMR spectrum of the virgin PVDF membrane was compared with that of the chelating membrane. Fig. 2 shows the spectra of PVDF membrane and the chelating membrane. As indicated in Fig. 2, the peaks at 20.1 ppm and 33.1 ppm originate from adamantane which is used as the internal standard. The $-\text{CH}_2-$ and $-\text{CF}_2-$ carbons of the PVDF main chains contribute to the peaks at 44.6 ppm and 121.8 ppm, consistent with the data that have been reported in literature [24]. In addition to the shared peaks, it is also observed that there appear several important differences between the spectra. The peak which appears at 56.0 ppm is assigned to $-\text{CH}_2\text{N}-$ carbon of DTPA and the peak at 158.7 ppm can be attributed to the three carbons in the triazine ring of melamine. The 168.5 ppm peak points to carbonyl carbon of amide or carboxylic groups [18]. Due to high intensity of the peak at 168.5 ppm, it can be assumed that the content of polyaminecarboxylate compounds is relatively high in the chelating membrane. Therefore, the polyaminecarboxylate groups with the functionality of chelation, as inferred from the ^{13}C solid-state NMR spectra, have been blended to PVDF membrane.

3.1.3. FTIR spectra

Fig. 3 presents the spectra of the virgin PVDF membrane, the chelating membrane, polyaminecarboxylate compounds and nickel-loaded compounds. As indicated in Fig. 3a, the peaks appearing at 471, 1200 and 3025 cm^{-1} derive from C–F wagging, bending and stretching vibration of PVDF polymer, respectively [25]. Com-

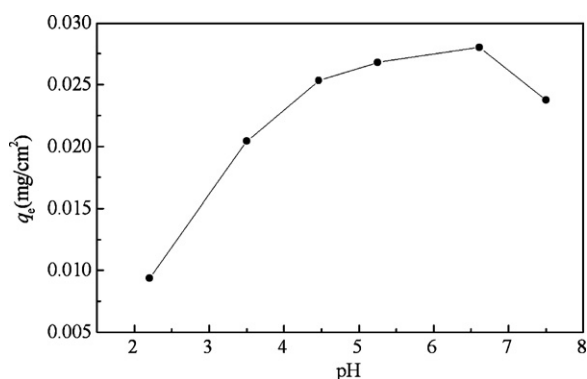


Fig. 4. Effect of pH on the adsorption of Ni(II) by the chelating membrane. $C_0(\text{Ni}) = 50 \text{ mg/L}$; t : 120 min; membrane area: 157 cm^2 ; temperature: 298 K.

paring curve a with b and c, one should observe several new peaks including 690 and 1636 cm^{-1} , which are due to the amide N–H out of plane and amide carbonyl C=O stretching, respectively. These two peaks support the formation of the amide covalent bonds between DTPA and melamine, indicating the polyaminocarboxylate functional groups have been blended to PVDF membrane. The peak at 1552 cm^{-1} is attributable to N–H bending of bridging secondary amine groups. As shown in Fig. 3c and d, the intensity of the peak at 1390 cm^{-1} related to carboxylic in plane O–H bending and the peak at 1636 cm^{-1} shows an observable decrease due to carboxylic O–H coordination. The decreasing intensity of the peak at 1205 cm^{-1} , which is as a result of C–N bonds weakening, is indicative that nitrogen atoms of DTPA skeleton are sites for complexation. The new broad peak at 1085 cm^{-1} in the vicinity of 1205 cm^{-1} also confirms the coordination of DTPA amino groups [26]. No identifiable change for the peak at 1552 cm^{-1} may mean the amide nitrogen atoms are free. Moreover, the weak peaks at 610 cm^{-1} may originate from Ni–N bond [18]. Thus, the chemical interactions during the adsorption process are evidenced by FTIR results. One can assume that the carboxylic and amino groups pertaining to DTPA coordinate to Ni(II), thereby forming complexes.

3.2. Effect of variables

3.2.1. Effect of pH

Adsorption of metal ions onto the chelating membrane is a pH dependent process. The influence of pH on the adsorption properties is shown in Fig. 4. The pH range studied varies from 2.0 to 7.5. As can be noticed, with increasing pH value, higher adsorption capacities can be obtained. The optimum pH for adsorption is located at 6.6. When the pH exceeds 7, the uptake decreases because the nickel ions start to precipitate as $\text{Ni}(\text{OH})_2$. According to the results of FTIR spectra, chelation may dominate in the adsorption process. At lower pH values, the functional groups for coordination including carboxylic and amine groups are protonated, which does not favor the chelation. On the other hand, the H^+ ions compete with Ni(II), which also decreases the uptake. When the pH increases, the chelation reaction tends to occur with the deprotonation of the functional groups for coordination.

3.2.2. Effect of Ca(II)

The occurrence of calcium ions is ubiquitous in wastewater effluents. The polyaminocarboxylate chelator tends to bind almost all the metal ions due to its high complexing capability. Therefore, Ca(II) ions may occupy the active sites for complexation to compete with Ni(II). The effect of Ca(II) ions is highly dependent on the relative complexation strength that the chelating membrane shows for Ca(II) and Ni(II) ions. In this respect, a series of adsorption experi-

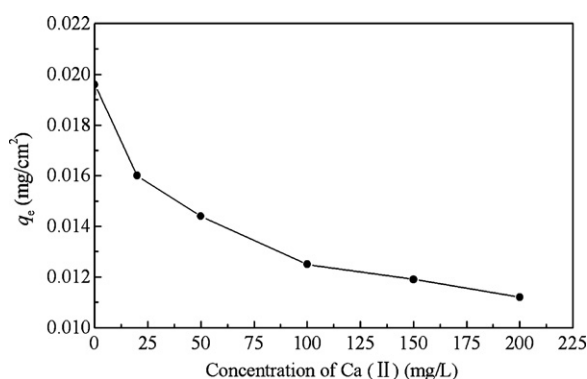


Fig. 5. Effect of Ca(II) on the adsorption of Ni(II) by the chelating membrane. $C_0(\text{Ni}) = 50 \text{ mg/L}$; t : 120 min; membrane area: 157 cm^2 ; temperature: 298 K; pH: 6.6.

ments were carried out to examine the interference of Ca(II) ions, with the initial Ni(II) concentration of 50 mg/L .

Fig. 5 shows the variation of Ni(II) uptake as a function of Ca(II) concentration. Table 1 gives out the distribution coefficient for Ni(II) and separation factor for Ni(II) and Ca(II) at different Ca(II) concentrations. At lower Ca(II) concentration, an identifiable change occurs to the Ni(II) uptake compared to the single nickel ions system. As the concentration of Ca(II) ions increases from 20 to 50 mg/L , the uptake decreases by 18–27%. For larger concentrations (100 – 200 mg/L), the increase of Ca(II) concentration has a moderate impact on the variation of Ni(II) uptake. When the concentration of Ca(II) is 200 mg/L , the reduction percentage of the adsorption capacity is 43%. As indicated in Table 1, the distribution coefficient ($K_{D(\text{Ni})}$) decreases from 4.27 to 2.72, and the separation factor ($f_{\text{Ni(II)/Ca(II)}}$) increases from 3.10 to 8.46 at increased Ca(II) concentrations (20 – 200 mg/L). This reveals that competitive adsorption exists in the sorption process with the simultaneous presence of Ni(II) and Ca(II) ions. What is more, nickel adsorption dominates over calcium ions, indicating that the chelating membrane shows more affinity and selectivity for Ni(II) than Ca(II) ions. Thus, the chelating membrane can be applied to treat the nickel plating wastewater containing calcium ions.

3.2.3. Effect of lactic acid

Lactic acid, as a chelating agent, is widely used in the nickel plating industries. With comparatively small stability constants, lactic acid is a weak chelating agent containing two coordination sites. The stronger complexation strength of the chelating membrane towards Ni(II) than lactic acid induces that the adsorption process experiences low steric hindrance which will otherwise hamper the Ni(II) uptake of the chelating membrane.

The adsorption profile for different lactic acid concentrations at pH 6.6 is shown in Fig. 6. The Ni(II) uptake decreases insignificantly with increasing lactic acid concentration. It is also should be noted that the profile tends to be more smooth at larger lactic acid concentrations. This may be because all the nickel ions are complexed and the crowding effect relating to the formation of nickel–lactic acid complexes is not promoted as the lactic acid concentration increases. In the range studied, the maximum decrease percentage of the uptake is 10%, which is located at the acid concentration of 10 mL/L . Consequently, with special respect to a potential applica-

Table 1

Distribution coefficient for Ni(II) and separation factor for Ni(II) and Ca(II) at different Ca(II) concentrations.

$C_0(\text{Ca})$ (mg/L)	0	20	50	100	150	200
$K_{D(\text{Ni})}$	5.66	4.27	3.72	3.11	2.93	2.72
$f_{\text{Ni(II)/Ca(II)}}$	–	3.10	4.78	5.85	7.56	8.46

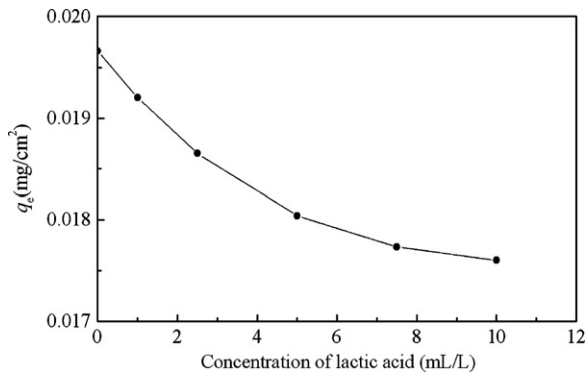


Fig. 6. Effect of lactic acid on the adsorption of Ni(II) by the chelating membrane. $C_0(\text{Ni}) = 50 \text{ mg/L}$; $t = 120 \text{ min}$; membrane area: 157 cm^2 ; temperature: 298 K ; $\text{pH} = 6.6$.

tion, this property facilitates the use of this chelating membrane to the recovery of nickel from organic acid complexes.

3.3. Adsorption studies

Adsorption kinetics and equilibrium, as the two important physicochemical aspects, play a significant role in parameterized evaluation of the sorption process. In this section, the adsorption characteristics of the chelating membrane towards Ni(II) were examined for the following three systems: (1) the single Ni(II) ions system, (2) the binary Ni(II) and Ca(II) system, (3) the Ni(II)–lactic acid complexes system. Some comparisons were made to interpret the influence of calcium ions and lactic acid on the adsorption kinetics and thermodynamics. Finally, the thermodynamic parameters, including ΔH° , ΔS° and ΔG° were calculated based on the experimental data.

3.3.1. Adsorption kinetics

Sorption kinetics, which is associated with solute uptake rate and determines the residence time of the adsorption reaction, is an important property defining the sorption efficiency [27]. Hence, experiments were performed to have a clear insight into the kinetics of nickel removal by the chelating membrane. The uptakes as a function of time for different temperatures are shown in Fig. 7. In the single nickel ions system, as inferred from Fig. 7a, the time required to achieve equilibrium is 60 min, which is used as the equilibration time for subsequent experiments. It can also be seen that two stages, including rapid and slow stage, occur in the nickel adsorption processes. The rapid stage extends for the first 10 min while the slow adsorption for the remaining 50 min. During the first 30 min, 85% of the total Ni(II) uptake has been attained for these three temperatures, displaying a fast adsorption characteristic of the chelating membrane.

As for the binary Ni(II) and Ca(II) system, Fig. 7b displays that the equilibrium time is shortened in addition to the uptake decrease. Consequently, the competitive adsorption of calcium ions can interfere with nickel sorption significantly and have an influence on the kinetics. From Fig. 7c, a decrease of the uptake can be also observed in nickel–lactic acid complexes system. In comparison with the single nickel adsorption, the equilibrium time shows no identifiable change. The binding strength of lactic acid is inconsiderable, compared to the polyaminocarboxylate groups of the chelating membrane.

In order to reveal the adsorption mechanism, the kinetic data under these three systems were fitted to Lagergren first-order, second-order equation and intraparticle diffusion model. The linear form of these three models can be written as follows [28]:

$$\text{First-order equation: } \ln(q_e - q_t) = \ln q_e - k_1 t \quad (5)$$

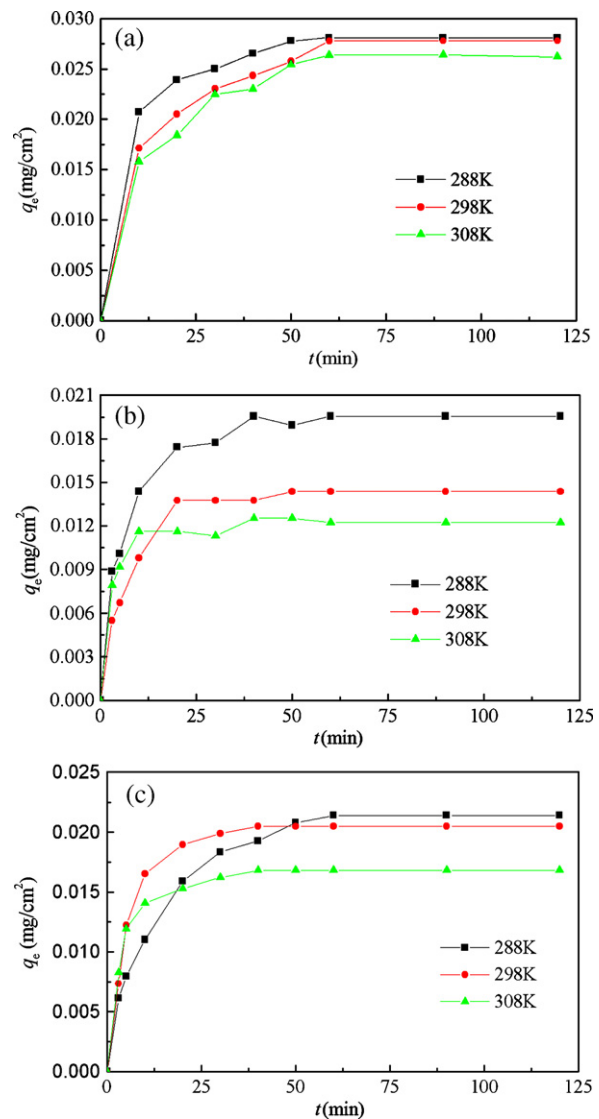


Fig. 7. Adsorption kinetics for Ni(II) on the chelating membrane in different systems: (a) the single Ni(II) ions system; (b) the binary Ni(II) and Ca(II) system; (c) the Ni(II)–lactic acid complexes system. $C_0(\text{Ni}) = 50 \text{ mg/L}$; $C_0(\text{Ca}) = 50 \text{ mg/L}$; $C_0(\text{lactic acid}) = 0.01 \text{ mol/L}$; $t = 120 \text{ min}$; membrane area: 157 cm^2 ; $\text{pH} = 6.6$.

$$\text{Second-order equation: } \frac{t}{q_t} = \frac{1}{k_2 q_e^2} + \frac{t}{q_e} \quad (6)$$

$$\text{Intraparticle diffusion model: } q_t = k_{id} t^{1/2} \quad (7)$$

where q_e and q_t are the amounts of adsorbed Ni(II) (mg/cm^2), at equilibrium and at time t , respectively. k_1 (min^{-1}), k_2 ($\text{cm}^2/(\text{mg min})$) and k_{id} ($\text{mg}/(\text{cm}^2 \text{min}^{1/2})$) are the rate constants.

The parameters of the three models are summarized in Table 2. As the correlation coefficient ($R^2 > 0.99$) indicates, Lagergren second-order model can be representative of the adsorption process, pointing to a chemical sorption character. What is more, the calculated uptake of equilibrium derived from the data fitting is consistent with the experimental adsorption capacity. Intraparticle diffusion equation, which can identify the diffusion mechanism, confirms that two stages occur as mentioned above. The rapid stage is due to the membrane diffusion where the intraparticle diffusion is the rate-limiting step. Comparatively, the slow stage is the equilibrium step where intraparticle diffusion starts to slow down. In conclusion, nickel ions are transported to the surface of the membrane via membrane diffusion and then intraparticle

Table 2
Adsorption kinetics parameters of the chelating membrane for Ni(II).

System	T (K)	Lagergren first-order model		Lagergren second-order model		Intraparticle diffusion model					
		k_1 (min^{-1})	q_e (mg/cm^2)	R^2	k_2 ($\text{cm}^2/(\text{mg}\cdot\text{min})$)	q_e (mg/cm^2)	R^2	k_{d1} ($\text{mg}/(\text{cm}^2\cdot\text{min}^{1/2})$)	R^2	k_{d2} ($\text{mg}/(\text{cm}^2\cdot\text{min}^{1/2})$)	R^2
Single nickel ions system	288	0.0597	0.0220	0.9478	3.293	0.0290	0.9984	0.0024	0.9814	0.0019	0.9989
	298	0.0617	0.0186	0.9605	4.171	0.0264	0.9971	0.0025	0.9880	0.0016	0.9860
	308	0.1086	0.0183	0.9559	7.694	0.0245	0.9955	0.0047	0.9958	0.0013	0.9785
Binary Ni(II) and Ca(II) system	288	0.0784	0.0142	0.9203	10.19	0.0211	0.9984	0.0045	0.9929	0.0007	0.7624
	298	0.1157	0.0128	0.9222	11.39	0.0159	0.9968	0.0037	0.9764	0.0002	0.7080
	308	0.9215	0.0053	0.7522	23.94	0.0127	0.9976	0.0031	0.9989	0.0003	0.7093
Ni(II)-lactic acid complexes system	288	0.0624	0.0194	0.9639	4.144	0.0242	0.9975	0.0035	0.9997	0.0017	0.9771
	298	0.1152	0.0166	0.9800	6.203	0.0216	0.9983	0.0053	0.9810	0.0005	0.8147
	308	0.1007	0.0109	0.9387	10.49	0.0174	0.9995	0.0046	0.9892	0.0005	0.8160

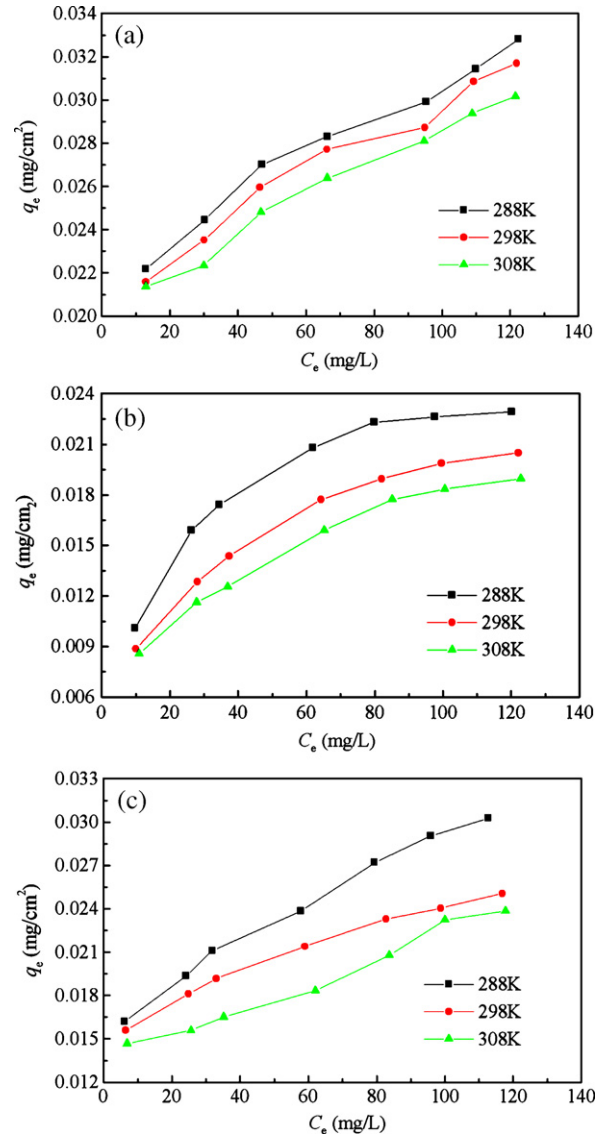


Fig. 8. Adsorption isotherm for Ni(II) on the chelating membrane in different systems: (a) the single Ni(II) ions system; (b) the binary Ni(II) and Ca(II) system; (c) the Ni(II)-lactic acid complexes system. $C_0(\text{Ca}) = 50 \text{ mg/L}$; $C_0(\text{lactic acid}) = 0.01 \text{ mol/L}$; $t: 120 \text{ min}$; membrane area: 157 cm^2 ; pH: 6.6.

diffusion facilitates the ions to retain on the complexation sites. As can be seen in Table 2, calcium ions presence affects Lagergren second-order rate constant. The rate constant is larger than that of single nickel ions system, indicating the competitive adsorption of calcium ions accelerates the sorption process and shortens the residence time. In the case of nickel-lactic acid complexes system, the formation of complexes has a considerable effect on the rate constants as the calcium ions does. This effect indicates the nature of solute is changed as the complexes form and this nature interferes in the kinetic process.

3.3.2. Equilibrium adsorption

Fig. 8 presents nickel adsorption isotherms as a function of the equilibrium concentration of nickel ions under three systems. It can be seen from Fig. 8a that the adsorption capacity decreases with the increasing temperature. Therefore, lower temperature favors the adsorption process. However, the temperature does not exert a significant influence on the adsorption capacity as the uptake shows no considerable difference among the three temperatures. As can be seen in Fig. 8b, the noticeably different trend of the isotherm

with the presence of calcium ions demonstrates that the calcium ions affect the nickel adsorption when the ionic strength or competitive adsorption are taken into consideration. Conversely, the effect caused by the addition of lactic acid on the adsorption isotherm, as can be noted in Fig. 8c, is insignificant despite of the formation of the nickel–lactic acid complexes.

Freundlich, Langmuir and D–R isotherm models were employed for adsorption data correlation to quantify the adsorption capacity of the membrane. The linear forms of these three models are listed as follows [29,30]:

$$\text{Freundlich model: } \ln q_e = \ln K_F + \frac{1}{n} \ln c_e \quad (8)$$

$$\text{Langmuir model: } \frac{c_e}{q_e} = \frac{1}{q_m b} + \frac{c_e}{q_m} \quad (9)$$

$$\text{D–R model: } \ln q_e = \ln q_m - k\varepsilon^2 \quad (10)$$

$$\varepsilon = RT \ln \left(1 + \frac{1}{c_e} \right) \quad (11)$$

$$E = \frac{1}{(2k)^{1/2}} \quad (12)$$

where q_e (mg/cm²) is the amount of adsorbed Ni(II) at equilibrium, c_e (mg/L) is the concentration of Ni(II) at equilibrium. K_F and n are associated with the adsorption capacity and adsorption intensity, respectively. Langmuir parameter b (L/mg) is related to the adsorption affinity. ε is Polanyi potential; E (kJ/mol) is the mean free energy of adsorption.

As Table 3 displays, because of the relatively high correlation parameters, the experimental data can be well described by the three models, in which the Langmuir model gives the best fit ($R^2 > 0.99$). In the single nickel component, Freundlich parameter, the K_F value, supports the order of nickel uptake is 288 K > 298 K > 308 K, which is confirmed by the corresponding $1/n$ values. Langmuir isotherm model is based on the assumption that the dynamic adsorption–desorption processes occur on homogeneous surface, taking no account of the interaction between the membrane and the solute. Thus, the adsorption of nickel on the membrane can be explained as mono-molecular layer of the adsorption. The calculated maximum adsorption capacities (q_m) are slightly greater than the experimental values regarding that there are still unoccupied adsorption sites. Moreover, the adsorption affinity (b) in the order of 288 K > 298 K > 308 K reflects that low temperature is more preferable for the nickel adsorption. The adsorption mechanism of nickel ions on the chelating membrane is predicted by D–R isotherm model. Values of E relating to the mean free energy of adsorption vary from 8 to 16 kJ/mol, which is indicative of the ion-exchange adsorption [30].

The isothermal parameters of the single nickel ions system are compared to that of the system with the presence of calcium ions and lactic acid, respectively. As indicated in Table 3, it is apparent that the presence of calcium ions affects the adsorption isotherm significantly, whereas lactic acid has a moderate effect on the isotherm. The higher $1/n$ values than that of single nickel ions system demonstrate that calcium ions interfere with nickel adsorption; the value of b reflects the same trend. However, in the nickel–lactic acid complexes, the values of $1/n$ and b associated with the adsorption capability exhibit no considerable difference. Hence, the chelating membrane can be applied to treat the nickel plating effluents without considerable loss of the uptake.

3.3.3. Thermodynamic parameters

Thermodynamic parameters, properly assessed, could provide detailed information with regard to the inherent energy. The final capacity of the membrane and the adsorption mechanism can

Table 3
Adsorption isotherm parameters of the chelating membrane for Ni(II).

System	T (K)	Freundlich model			Langmuir model			D–R model		
		K_F	$1/n$	R^2	q_m (mg/cm ²)	b (L/mg)	R^2	q_m (mg/cm ²)	E (kJ/mol)	R^2
Single nickel ions system	288	0.0168	0.2766	0.9634	0.0370	0.0923	0.9936	0.0548	15.21	0.9931
	298	0.0150	0.2824	0.9790	0.0364	0.0871	0.9944	0.0515	15.81	0.9746
	308	0.0148	0.2841	0.9886	0.0357	0.0826	0.9921	0.0493	15.91	0.9974
Binary Ni(II) and Ca(II) system	288	0.0051	0.3294	0.9601	0.0263	0.0608	0.9991	0.0578	11.32	0.9773
	298	0.0041	0.3355	0.9932	0.0240	0.0457	0.9957	0.0512	11.47	0.9966
	308	0.0037	0.3411	0.9944	0.0225	0.0412	0.9918	0.0467	11.85	0.9915
Ni(II)–lactic acid complexes system	288	0.0092	0.2623	0.9747	0.0337	0.0927	0.9840	0.0566	12.95	0.9571
	298	0.0085	0.2699	0.9740	0.0266	0.0723	0.9945	0.0421	14.87	0.9724
	308	0.0078	0.2747	0.9399	0.0256	0.0684	0.9866	0.0395	14.94	0.9146

Table 4
Adsorption thermodynamic parameters of the chelating membrane for Ni(II).

System	ΔH° (kJ/mol)	ΔS° (kJ/mol K)	T (K)	ΔG° (kJ/mol)	R^2
Single nickel ions system	-11.11	0.0149	288	-15.41	0.9964
			298	-15.56	
			308	-15.71	
Binary Ni(II) and Ca(II) system	-20.86	0.0005	288	-21.00	0.9630
			298	-21.01	
			308	-21.02	
Ni(II)-lactic acid complexes system	-12.90	0.0300	288	-21.54	0.9340
			298	-21.84	
			308	-22.14	

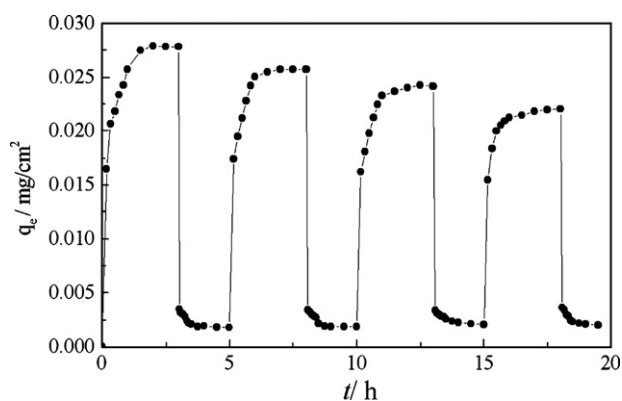


Fig. 9. Repeated adsorption/desorption curve for the chelating membrane towards Ni(II).

also be evaluated based on these parameters [31]. These parameters including the standard free energy change (ΔG°), standard enthalpy change (ΔH°), and standard entropy change (ΔS°) were calculated and summarized in Table 4 [32].

$$\ln K_D = -\frac{\Delta H^\circ}{RT} + \frac{\Delta S^\circ}{R} \quad (13)$$

$$\Delta G^\circ = \Delta H^\circ - T \Delta S^\circ \quad (14)$$

where K_D is the distribution coefficient (mL/m^2), and R is the gas constant. It can be seen from Table 4 that the values of ΔH° are negative, indicating the exothermic nature of the adsorption process. This is reasonable as the adsorption capacity decreases with increasing temperature. The positive entropy change shows the increasing randomness during the adsorption process, in which the hydrated nickel ions tend to liberate water molecules. This liberation is essential for the occurrence of the chelation reaction, promoting the disorder of the system. The standard Gibbs free energy change displays negative values under all systems, which means that the adsorption process is spontaneous.

3.4. Desorption of the chelating membrane

Taking account of the reuse of the chelating membrane, the adsorption/desorption property of the membrane is fundamental for practical applications. As mentioned above, the chelation reaction is not favored at lower pH values. Through experimental estimation, 1 mol/L HCl solution was thereby used to regenerate the membrane. Fig. 9 depicts the adsorption/desorption curves of four cycles. It can be recognized that the adsorption capacity of the membrane is better maintained after four cycles of the adsorption/desorption processes. The total uptake still exceeds 0.022 mg/cm² and the desorption efficiency is more than 90%. Therefore, the membrane can be repeatedly used without significant loss of the uptake.

4. Conclusion

The PVDF chelating membrane was synthesized via the covalent amide bond between DTPA and melamine to form polyaminocarboxylate compounds. The adsorption performances of prepared membrane were measured under three conditions: the single Ni(II) system, binary Ni(II) and Ca(II) system and nickel-lactic acid complexes system. The conclusions are shown below.

- (1) SEM elucidates that the surface of the chelating membrane is still composed of a microporous structure with identifiable difference from that of the virgin membrane. NMR and FTIR confirm the successful blending of polyaminocarboxylate groups to PVDF membrane. FTIR also shows that chemical bonding exists in the adsorption process.
- (2) The optimum pH for adsorption is 6.6 and the contact time required to achieve equilibrium is 60 min. Increasing the concentration of Ca(II) induces a considerable change in adsorption capacity of Ni(II). The distribution coefficient of Ni(II) ($K_{D(\text{Ni})}$) decreases from 4.27 to 2.72, and the separation factor ($f_{\text{Ni(II)/Ca(II)}}$) increases from 3.10 to 8.46 when the initial Ca(II) concentration varies from 20 to 200 mg/L. This reveals that nickel adsorption dominates over calcium ions, and the chelating membrane shows more affinity and selectivity for Ni(II) than Ca(II) ions. In the studied range of lactic acid concentration, the uptake decreases with the maximum ratio of 10%. Therefore, the chelating membrane can be applied to treat the nickel plating wastewater containing coexisting cations and organic chelating agents.
- (3) Lagergren second-order equation can represent sorption of Ni(II) onto the chelating membrane, indicating the chemisorption nature. This property is confirmed by the Langmuir and D-R models which fit well to the equilibrium data. The adsorption process is spontaneous ($\Delta G^\circ < 0$) and exothermic ($\Delta H^\circ < 0$). Ca(II) ions compete with Ni(II) for the same sorption sites, inducing the change of rate constant and equilibrium uptake in the binary mixture. The relatively weak binding ability of lactic acid towards Ni(II) does not affect the sorption characteristics significantly. This result means that the chelating membrane is capable of recovering nickel from wastewater effluents. In addition to lactic acid, citric acid and succinic acid are also the commonly used chelating agents. A further research will include the effect of these chelating agents with respect to the size and stability of these nickel-organic complexes. The treatment of spent solution from nickel plating will be also considered.
- (4) When the nickel-loaded membrane was immersed in 1 mol/L HCl solution to liberate Ni(II), the desorption efficiency still exceeds 90% after four cycles of adsorption/desorption operations.

References

- [1] K.E. Giller, E. Witter, S.P. McGrath, Toxicity of heavy metals to microorganisms and microbial processes in agricultural soils: a review, *Soil Biol. Biochem.* 30 (1998) 1389–1414.
- [2] M. Ajmal, A.H. Khan, S. Ahmad, A. Ahmad, Role of sawdust in the removal of copper(II) from industrial wastes, *Water Res.* 32 (1998) 3085–3091.
- [3] J.O. Nriagu, J.M. Pacyna, Quantitative assessment of worldwide contamination of air water, and soils by trace metals, *Nature* 333 (1988) 134–139.
- [4] L. Charemtanyarak, Heavy metals removal by chemical coagulation and precipitation, *Water Sci. Technol.* 39 (1999) 135–138.
- [5] G. Borbély, E. Nagy, Removal of zinc and nickel ions by complexation–membrane filtration process from industrial wastewater, *Desalination* 240 (2009) 218–226.
- [6] J. Aguado, J.M. Arsuaga, A. Arencibia, M. Lindo, V. Gascón, Aqueous heavy metals removal by adsorption on amine-functionalized mesoporous silica, *J. Hazard. Mater.* 163 (2009) 213–221.
- [7] P.G. Priya, C.A. Bashab, V. Ramamurthi, S.N. Begum, Recovery and reuse of Ni(II) from rinsewater of electroplating industries, *J. Hazard. Mater.* 163 (2009) 899–909.
- [8] A. Heidari, H. Younesi, Z. Mehraban, Removal of Ni(II), Cd(II), and Pb(II) from a ternary aqueous solution by amino functionalized mesoporous and nano mesoporous silica, *Chem. Eng. J.* 153 (2009) 70–79.
- [9] H.D. Doan, A. Lohi, V.B.H. Dang, T. Dang-Vu, Removal of Zn⁺² and Ni⁺² by adsorption in a fixed bed of wheat straw, *Process Saf. Environ.* 86 (2008) 259–267.
- [10] A. Smara, R. Delimi, E. Chainet, J. Sandeaux, Removal of heavy metals from diluted mixtures by a hybrid ion-exchange/electrodialysis process, *Sep. Purif. Technol.* 57 (2007) 103–110.
- [11] A. García-Sánchez, A. Alastuey, X. Querol, Heavy metal adsorption by different minerals: application to the remediation of polluted soils, *Sci. Total Environ.* 242 (1999) 179–188.
- [12] M.M. Nasef, A.H. Yahaya, Adsorption of some heavy metal ions from aqueous solutions on Nafion 117 membrane, *Desalination* 249 (2009) 677–681.
- [13] B. Yu, Y. Zhang, A. Shukla, S.S. Shukla, K.L. Dorris, The removal of heavy metals from aqueous solutions by sawdust adsorption—removal of copper, *J. Hazard. Mater.* 80 (2000) 33–42.
- [14] S. Bassaid, M. Chaib, A. Bouguelia, M. Trari, Elaboration and characterization of poly (acrylic acid-co-crotonic acid) copolymers: application to extraction of metal cations Pb(II), Cd(II) and Hg(II) by complexation in aqueous media, *React. Funct. Polym.* 68 (2008) 483–491.
- [15] A. Baraka, P.J. Hall, M.J. Heslop, Melamine–formaldehyde–NTA chelating gel resin: synthesis, characterization and application for copper(II) ion removal from synthetic wastewater, *J. Hazard. Mater.* 140 (2007) 86–94.
- [16] H.A. Abd El-Rehim, E.A. Hegazy, A. El-Hag Ali, Selective removal of some heavy metal ions from aqueous solution using treated polyethylene-g-styrene/maleic anhydride membranes, *React. Funct. Polym.* 43 (2000) 105–116.
- [17] L. Lebrun, F. Vallée, B. Alexandre, Q.T. Nguyen, Preparation of chelating membranes to remove metal cations from aqueous solutions, *Desalination* 207 (2007) 9–23.
- [18] A. Baraka, P.J. Hall, M.J. Heslop, Preparation and characterization of melamine formaldehyde DTPA chelating resin and its use as an adsorbent for heavy metals removal from wastewater, *React. Funct. Polym.* 67 (2007) 585–600.
- [19] R. Rojas, M.R. Perez, E.M. Erro, P.I. Ortiz, M.A. Ulibarri, C.E. Giacomelli, EDTA modified LDHs as Cu²⁺ scavengers: removal kinetics and sorbent stability, *J. Colloid Interface Sci.* 331 (2009) 425–431.
- [20] Y.J. Jiang, Q.M. Gao, H.G. Yu, Y.R. Chen, F. Deng, Intensively competitive adsorption for heavy metal ions by PAMAM-SBA-15 and EDTA-PAMAM-SBA-15 inorganic–organic hybrid materials, *Micropor. Mesopor. Mater.* 103 (2007) 316–324.
- [21] E. Repo, T.A. Kurniawan, J.K. Warchol, M.E.T. Sillanpää, Removal of Co(II) and Ni(II) ions from contaminated water using silica gel functionalized with EDTA and/or DTPA as chelating agents, *J. Hazard. Mater.* 171 (2009) 1071–1080.
- [22] K. Rezaei, H. Nedjate, Diluent effect on the distribution ratio and separation factor of Ni(II) in the liquid–liquid extraction from aqueous acidic solutions using dibutylthiophosphoric acid, *Hydrometallurgy* 68 (2003) 11–21.
- [23] T. Boccaccio, A. Bottino, G. Capannelli, P. Piaggio, Characterization of PVDF membranes by vibrational spectroscopy, *J. Membr. Sci.* 210 (2002) 315–329.
- [24] G.M. Qiu, L.P. Zhu, B.K. Zhu, Y.Y. Xu, G.L. Qiu, Grafting of styrene/maleic anhydride copolymer onto PVDF membrane by supercritical carbon dioxide: preparation, characterization and biocompatibility, *J. Supercrit. Fluid* 45 (2008) 374–383.
- [25] L.Z. Song, C.Y. Dong, J. Li, Application of the PAA–PVDF microfiltration composite membrane for municipal wastewater advanced treatment, *Toxicol. Environ. Chem.* 89 (2007) 223–232.
- [26] V.L. Silva, R. Carvalho, M.P. Freitas, C.F. Tormena, W.C. Melo, Structural determination of Zn and Cd–DTPA complexes: MS, infrared, ¹³C NMR and theoretical investigation, *Spectrochim. Acta A* 68 (2007) 1197–1200.
- [27] F. Gode, E. Pehlivan, A comparative study of two chelating ion-exchange resins for the removal of chromium(III) from aqueous solution, *J. Hazard. Mater.* 100 (2003) 231–243.
- [28] D.D. Milenković, P.V. Dašić, V.B. Veljković, Ultrasound-assisted adsorption of copper(II) ions on hazelnut shell activated carbon, *Ultrason. Sonochem.* 16 (2009) 557–563.
- [29] M.V. Dinu, E.S. Dragan, Heavy metals adsorption on some iminodiacetate chelating resins as a function of the adsorption parameters, *React. Funct. Polym.* 68 (2008) 1346–1354.
- [30] B.P. Bering, M.M. Dubinin, V.V. Serpinsky, On thermodynamics of adsorption in micropores, *J. Colloid Interface Sci.* 38 (1972) 185–194.
- [31] A. Ramesh, D.J. Lee, J.W.C. Wong, Thermodynamic parameters for adsorption equilibrium of heavy metals and dyes from wastewater with low-cost adsorbents, *J. Colloid Interface Sci.* 291 (2005) 588–592.
- [32] D. Mohan, K.P. Singh, Single- and multi-component adsorption of cadmium and zinc using activated carbon derived from bagasse—an agricultural waste, *Water Res.* 36 (2002) 2304–2318.